CONFIDENTIAL

Copy 331
RM L53G29a

NACA RM L53G29a

NACA

RESEARCH MEMORANDUM

DAMPING-IN-PITCH CHARACTERISTICS AT HIGH SUBSONIC AND TRANSONIC SPEEDS OF FOUR 35° SWEPTBACK WINGS

By William B. Kemp, Jr., and Robert E. Becht

Langley Aeronautical Laboratory
Langley Field, Va.

CLASSIFIED DOCUMENT

This material contains information affecting the National Defense of the United States within the meaning of the espionage laws, Title 18, U.S.C., Secs. 793 and 794, the transmission or revelation of which in any manner to an unauthorized person is prohibited by law.

NATIONAL ADVISORY COMMITTEE
FOR AERONAUTICS

WASHINGTON
October 16, 1953

CONFIDENTIAL

NATIONAL ADVISORY COMMITTEE FOR AERONAUTICS

RESEARCH MEMORANDUM

DAMPING-IN-PITCH CHARACTERISTICS AT HIGH SUBSONIC AND TRANSONIC SPEEDS OF FOUR 35° SWEPTBACK WINGS

By William B. Kemp, Jr., and Robert E. Becht

SUMMARY

Free-oscillation tests in pitch have been made with angles of attack near zero on four semispan-wing models having an aspect ratio of 3.0, a taper ratio of 0.6, and 35° sweepback of the quarter-chord line. Thickness ratios of 6 percent and 10.5 percent were investigated and two model sizes were used. The highest test Mach number for the larger models was 0.97 with a Reynolds number of about 4×10^6; whereas, the small models were tested at Mach numbers up to 1.05 and Reynolds numbers of about 0.5×10^6. The effects of leading-edge roughness were determined for each model.

The results indicated that a marked loss of damping in pitch usually occurred at transonic speeds. The small-model results, which showed poor agreement with the large-model results at lower speeds, indicated that the damping reached a minimum at about Mach number 1.0 and tended to improve at higher speeds. A strong tendency was observed for a reciprocal relation to exist between the restoring moment and the damping at transonic speeds; that is, an increase in restoring moment was accompanied by a decrease in damping. Buffeting occurred at angles of attack near zero and Mach numbers above 0.91 on the large thick wing but was not observed on the thin wing.

INTRODUCTION

Recent increases in aircraft flight speeds and altitudes have caused increasing difficulty in the attainment of satisfactory damping of longitudinal oscillations. The low air density encountered at high altitudes leads to low aerodynamic damping forces. Also, small changes in Mach number at transonic speeds often produce large changes in the aerodynamic parameters affecting the longitudinal motions. In addition, some unconventional configurations used for high-speed aircraft have inherently poor longitudinal damping characteristics. Cases have been observed in

flight both of rocket-propelled research vehicles (ref. 1) and of piloted aircraft in which continuous longitudinal oscillations, or porpoising, occurred at transonic speeds. A collection of the results of damping-in-pitch measurements made in flight on a number of rocket-propelled research vehicles and piloted aircraft is presented in reference 2. These results indicate that the damping in pitch is likely to be very erratic and unpredictable at transonic speeds. A more fundamental study is needed, therefore, to isolate the effects of individual variables on damping in pitch. One approach to such a study is contained in reference 3 which presents a useful theoretical treatment of the damping in pitch of wings supported by experimental results at subsonic and supersonic speeds. The Mach number range from 0.9 to 1.2, however, is not treated in reference 3. An experimental study has been initiated in the Langley high-speed 7- by 10-foot tunnel in which an attempt is made to obtain damping-in-pitch information at low lift coefficients in the transonic speed range. Some results showing effects of thickness ratio, Reynolds number, and leading-edge roughness are presented in this paper.

The results presented were obtained from free-oscillation pitching tests of four semispan-wing models, all of which had an aspect ratio of 3.0, a taper ratio of 0.6, and 35° sweepback of the quarter-chord line. Thickness ratios of 6 percent and 10.5 percent were investigated and two model sizes were used. The highest test Mach number for the large models was 0.97 with a Reynolds number of about 4×10^6; whereas, the small models were tested at Mach numbers up to 1.05 and Reynolds numbers of about 0.5×10^6. The effects of leading-edge roughness were determined for each model.

SYMBOLS

C_m pitching-moment coefficient, $\dfrac{\text{Pitching moment}}{\frac{1}{2}\rho V^2 S\bar{c}}$

$C_{m_\alpha} = \dfrac{\partial C_m}{\partial \alpha}$

$C_{m_{\dot{\alpha}}} = \dfrac{\partial C_m}{\partial \dot{\alpha}\bar{c}/2V}$

$C_{m_q} = \dfrac{\partial C_m}{\partial q\bar{c}/2V}$

$\frac{\omega c}{2V}$	reduced frequency of oscillation
c	local wing chord, ft
$\bar{c}$	mean aerodynamic chord, ft
f	frequency of oscillation, cps
I_y	moment of inertia of oscillating mass about pitching axis, slug-ft^2
k	spring rate, ft-lb/radian
M	test Mach number
M_l	local Mach number
q	pitching velocity, $\frac{\partial \theta}{\partial(\text{time})}$, radian/sec
R	Reynolds number
S	area of (semispan) wing, sq ft
t	maximum thickness of airfoil section, ft
V	free-stream velocity, ft/sec
α	angle of attack, radians
$\dot{\alpha}$	rate of change of angle of attack, $\frac{\partial \alpha}{\partial(\text{time})}$, radian/sec
λ	logarithmic decrement, $\frac{d(\log \theta_o)}{d(\text{time})}$, per second
ρ	free-stream mass density of air, slugs/cu ft
θ	pitch attitude, radians or deg
θ_o	half-amplitude of oscillation, deg
ω	circular frequency, $2\pi f$, radian/sec

MODEL AND APPARATUS

Four semispan-wing models, differing only in size and thickness ratio, were used in the investigation. Pertinent dimensions of the models are given in figure 1. The airfoil sections of the thick models, taken perpendicular to the quarter-chord line, were NACA 0012-63 modified behind the 0.40 chord point to incorporate a slight cusp at the trailing edge. The resulting thickness ratio in the streamwise direction was 10.5 percent. The airfoil sections of the thin models were proportionately reduced to provide a 6-percent streamwise thickness ratio. Coordinates of both airfoil sections are given in table I. For the tests of the large models with leading-edge roughness, No. 60 carborundum particles were applied to the upper and lower surfaces over the forward 10 percent chord. A smaller grain roughness was used for the small models. For one test, the large thick model was fitted with trailing-edge strips 1/16 inch thick and 3/8 inch wide fastened on both surfaces so that the downstream edges of the strips were flush with the trailing edge (see fig. 1).

The models were so constructed that the stiffness was relatively independent of thickness ratio. The large models were of composite wood and metal construction and the small models were machined from steel and duralumin for the thin and thick models, respectively.

For both the large and small models, the pitching axis was located at $0.17\bar{c}$. Freedom in pitch about this axis was provided by a system of flexures located in the model support structure. This flexure system also provided the only spring restraint used in the tests. The model motions were recorded on film by use of an optical system which reflected a light beam from a mirror mounted on the model support system so that a time history of the model pitch angle was obtained.

The small models were tested in conjunction with a reflection plane which was spaced out from the tunnel wall to bypass the tunnel boundary layer. Blockage of the reflection plane and its support produced sufficient local velocity over the surface of the reflection plane to allow tests at Mach numbers up to 1.05 without choking the tunnel. The resulting flow field is shown in figure 2 by Mach number contours in the model chord plane for several tunnel speeds. The small models were fitted with $2\frac{1}{2}$-inch-diameter circular-root end plates which were recessed into the reflection plane to provide a smooth reflection-plane surface. The clearance between the end plate and the reflection plane was kept small to minimize flow leakage around the model root.

For the large models, the tunnel wall served as a reflection plane. Each large model was fitted with an end plate which projected 1 inch from

the model surface at the root. The models were installed so that the end plate was spaced about 1/16 inch from the tunnel wall. In addition, a 5-section labyrinth seal was installed outside the tunnel to restrict air leakage through the wall at the model root and still allow freedom for the models to perform pitching oscillations.

TEST TECHNIQUE AND REDUCTION OF DATA

Similar test techniques were used for both model sizes. The spring constant of the flexure supports was determined by measurement of the model displacements resulting from a series of applied pitching moments. These measurements were made both before and after the entire series of tests of each model size. Wind-off motion records were made before and after the wind-on tests of each model configuration by recording the motions after release from an initial manual displacement of about 3°. The method of obtaining wind-on records depended on the behavior of the model. If stability existed, the free motions following release from a displacement of about 3° were recorded continuously until the oscillation amplitude became either very small or relatively constant. If instability existed, the model was released with zero displacement and the ensuing buildup of oscillation was recorded until the half amplitude reached about 3°. In some cases, the existence of stability depended on the oscillation amplitude. For such cases, records were taken with several values of initial displacement to define the model behavior at any value of half amplitude less than 3°. At least two records were made at each test Mach number in order to provide an indication of experimental scatter. All tests were made with a mean angle of attack of zero.

From each record, the frequency of oscillation and the variation of amplitude θ_o with time were determined. The value of the logarithmic decrement $\lambda = \dfrac{d(\log \theta_o)}{d(\text{time})}$ was then measured from a faired plot of $\log \theta_o$ plotted against time. The following formulas were then used to obtain the results presented:

$$C_{m_q} + C_{m_{\dot{\alpha}}} = \frac{4I_y V}{qS\bar{c}^2}(\lambda - \lambda_o)$$

$$C_{m_\alpha} = \frac{k - \omega^2 I_y}{qS\bar{c}}$$

where

$$I_y = \frac{k}{\omega_o^2}$$

and λ_o and ω_o refer to wind-off values.

Corrections for model blockage have been applied to the Mach number of the large-model tests but no other jet-boundary corrections have been applied. It is believed that the tunnel resonance phenomenon discussed in reference 4 had no appreciable effect on the results of the present tests because, for the large models, the test frequency was always less than one-third the resonant frequency and, for the small models, the nonuniformity of the velocity field in the test section combined with the very small model size should render the resonance effect unimportant.

RESULTS AND DISCUSSION

The variation of Reynolds number with Mach number is presented for average test conditions for both the large and small models in figure 3. The Reynolds number of the small-model tests is so low that laminar separation may be expected to occur under certain conditions. Consequently, the usefulness of the small-model results is probably limited to qualitative illustration of the effects of increasing the Mach number above 0.97, the limit of the large-model tests.

The dynamic characteristics of the large models and the damping parameter of the small models are presented in figure 4. Values of the reduced frequency are also presented. The large-model results show essentially no effect of wing thickness, leading-edge roughness, or trailing-edge strips on the damping coefficient $C_{m_q} + C_{m_{\dot{\alpha}}}$ at Mach numbers below 0.85.

The damping of the large thin wing (figs. 4(a) and 4(b)) reached a maximum at about 0.9 Mach number and decreased sharply as the Mach number was increased to 0.97. The restoring moment coefficient C_{m_α} was essentially constant for Mach numbers below 0.9 but rapidly became more negative at higher Mach numbers indicating a rearward movement of the center of pressure as the Mach number increased. Leading-edge roughness had practically no effect on the damping or restoring moments of this wing.

The large thick wing with smooth leading edge (fig. 4(c)) exhibited appreciable scatter in the damping parameter at high Mach numbers. For this reason the damping curve was not faired in this range. The scatter

is attributed to buffeting which is discussed in more detail in a subsequent section of this paper. The results indicate that a significant loss of damping, similar to that observed with the thin wing, occurred at Mach numbers above 0.9. The restoring moment coefficient was more negative than that for the thin wing. Adding leading-edge roughness to the thick wing (fig. 4(d)) caused a rapid increase in damping as the Mach number approached 0.91. At higher speeds, a static instability at low angles of attack occurred together with buffeting which made the damping records impossible to analyze. Visual inspection of the records, however, indicated that the damping remained high at Mach numbers up to 0.93, the limit of this test. Unpublished results of exploratory forced-oscillation tests of this wing have shown large damping at Mach numbers up to 0.96. Adding trailing-edge strips to the thick wing with smooth leading edge (fig. 4(e)) caused a negative increment of C_{m_α} at all speeds. Only minor changes in the damping characteristics were produced except that a definite effect of amplitude was observed at Mach numbers above 0.93. Diverging oscillations occurred when the initial half amplitude was greater than 1.5°, whereas for smaller amplitudes the oscillations decayed.

The small-model damping results presented in figures 4(a) to 4(d) show very poor agreement with the corresponding large-model characteristics. The small thin wing with smooth leading edge (fig. 4(a)) showed especially poor agreement with the large model and is probably useful only in illustrating the possible magnitude of the effects of reducing Reynolds number. Similar reductions in damping with decreasing Reynolds number are illustrated in reference 5 for a 6-percent-thick triangular wing with free transition. Such reductions were not observed with fixed transition in reference 5.

Some significant trends are evident in the remaining small-model results (figs. 4(b) to 4(d)). The large loss of damping with increasing Mach number started at about the same Mach number as for the large models and continued to a Mach number of about 1.0 at which point the damping parameter was small or positive. At higher speeds the damping tended to level off or even improve indicating the possibility that no further loss of damping would occur at higher speeds.

In reference 2 it is pointed out that wings of 45° sweep or less typically exhibit an erratic variation of damping with Mach number in the transonic speed range. The present small-model results support this finding. Reference 2 states also that, if theoretical estimates of the damping are made at subsonic and at supersonic speeds and are faired smoothly through the transonic range, the resulting transonic damping estimates are likely to be optimistic. For the wing configurations examined in the present tests, there appears to be a strong tendency toward a reciprocal relation between the restoring and damping moments in the transonic speed range; that is, a decrease in damping is associated

with an increase in restoring moment. It is possible that recognition of this relation between damping and restoring moments may allow more realistic estimation of the transonic damping of a particular configuration if experimental static-stability data are available. The existence of this relation was not investigated for configurations other than those reported in this paper.

During the course of the free-oscillation tests of the large models it became apparent that the behavior of the thick wing at high Mach numbers was much more erratic than that of the thin wing. This difference in behavior is illustrated by the motion records presented in figure 5. The motion of the thin wing (fig. 5(a)) following a disturbance decayed in a fairly regular manner to very small residual amplitudes at all Mach numbers. The thick wing, however, (fig. 5(b)) at Mach numbers of 0.91 and greater, exhibited residual oscillations of randomly varying amplitude. In order for this type of motion to occur, the model must have been subjected to a fluctuating aerodynamic moment or buffeting. Adding trailing-edge strips (fig. 5(c)) considerably reduced the severity of the buffeting.

The computation of the damping coefficient from a test record is based on the assumption that no forcing moment is applied to the model during the time covered by the part of the record being analyzed. The existence of buffeting obviously introduces a forcing moment and may, therefore, cause the calculated damping coefficients to be in error. The records of figure 5(b) for $M = 0.91$ and 0.97, for example, show a buildup of oscillation amplitude from which a positive, or unstable, damping coefficient was calculated. It is possible, however, that the damping may have been stable and the observed oscillations were merely the response of the model to the buffeting excitation.

CONCLUSIONS

From the results of free-oscillation pitching tests of four wing models having an aspect ratio of 3.0 and 35° sweepback, the following conclusions are drawn:

1. In general, the model configurations tested showed a marked loss of damping in pitch at transonic speeds.

2. A strong tendency was observed for a reciprocal relation to exist between the restoring moment and the damping at transonic speeds; that is, an increase in restoring moment was accompanied by a decrease in damping.

3. Damping results obtained at a Reynolds number of about 0.5×10^6 were in poor agreement with those obtained on larger models at a Reynolds number of about 4×10^6.

4. The lower Reynolds number results indicated that minimum damping occurred at about Mach number 1.0. As Mach number was increased from 1.0, the damping tended to improve slightly. Higher Reynolds number results were not available at these Mach numbers.

5. Buffeting occurred at angles of attack near zero and Mach numbers above 0.91 on the 10.5-percent-thick wing but was not observed on the 6-percent-thick wing.

Langley Aeronautical Laboratory,
National Advisory Committee for Aeronautics,
Langley Field, Va., August 10, 1953.

REFERENCES

1. D'Aiutolo, Charles T., and Parker, Robert N.: Preliminary Investigation of the Low-Amplitude Damping in Pitch of Tailless Delta- and Swept-Wing Configurations at Mach Numbers From 0.7 to 1.35. NACA RM L52G09, 1952.

2. Gillis, Clarence L., and Chapman, Rowe, Jr.: Summary of Pitch-Damping Derivatives of Complete Airplane and Missile Configurations As Measured in Flight at Transonic and Supersonic Speeds. NACA RM L52K20, 1953.

3. Tobak, Murray: Damping in Pitch of Low-Aspect-Ratio Wings at Subsonic and Supersonic Speeds. NACA RM A52L04a, 1953.

4. Runyan, Harry L., Woolston, Donald S., and Rainey, A. Gerald: A Theoretical and Experimental Study of Wind-Tunnel-Wall Effects on Oscillating Air Forces for Two-Dimensional Subsonic Compressible Flow. NACA RM L52I17a, 1953.

5. Beam, Benjamin H.: The Effects of Oscillation Amplitude and Frequency on the Experimental Damping in Pitch of a Triangular Wing Having an Aspect Ratio of 4. NACA RM A52G07, 1952.

TABLE I

COORDINATES OF AIRFOIL SECTIONS

[All dimensions in percent of streamwise wing chord]

Station	Upper- and lower-surface ordinates	
	Thick wing	Thin wing
0	0	0
.587	1.096	.628
.880	1.323	.759
1.466	1.669	.956
2.926	2.260	1.296
5.830	2.998	1.719
8.710	3.492	2.002
11.568	3.863	2.215
17.215	4.393	2.520
22.773	4.752	2.723
28.241	4.995	2.862
33.620	5.149	2.952
38.912	5.232	3.000
44.116	5.220	2.992
49.234	5.130	2.940
54.265	4.909	2.816
59.212	4.551	2.609
64.074	4.078	2.338
68.959	3.532	2.025
73.546	2.955	1.694
78.158	2.382	1.366
82.688	1.839	1.054
87.137	1.338	.767
91.504	.876	.502
95.792	.441	.253
100.000	.021	.012

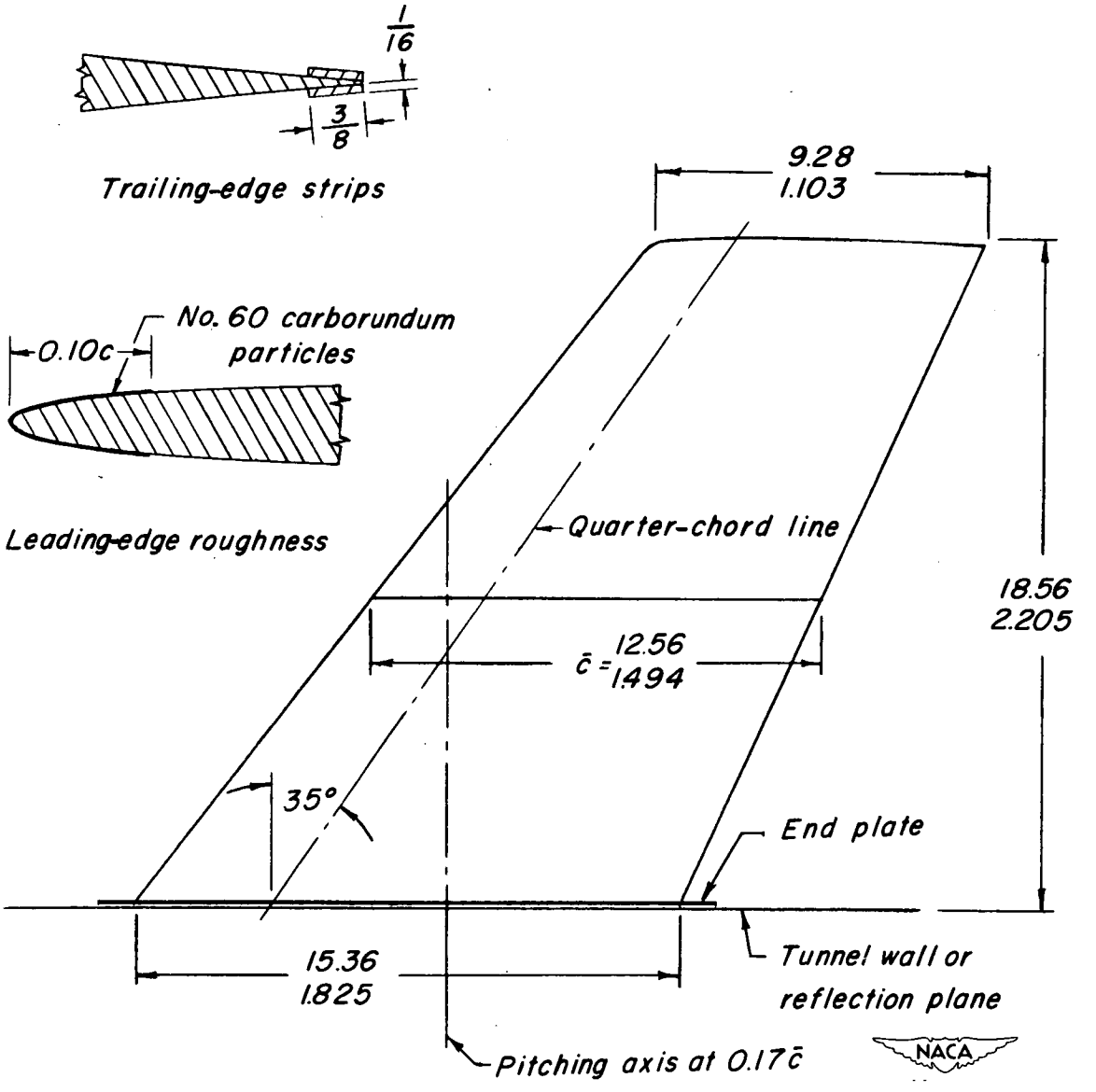

Figure 1.- Dimensions of test models. Two values given for the same dimension pertain to the two model sizes. All dimensions are in inches.

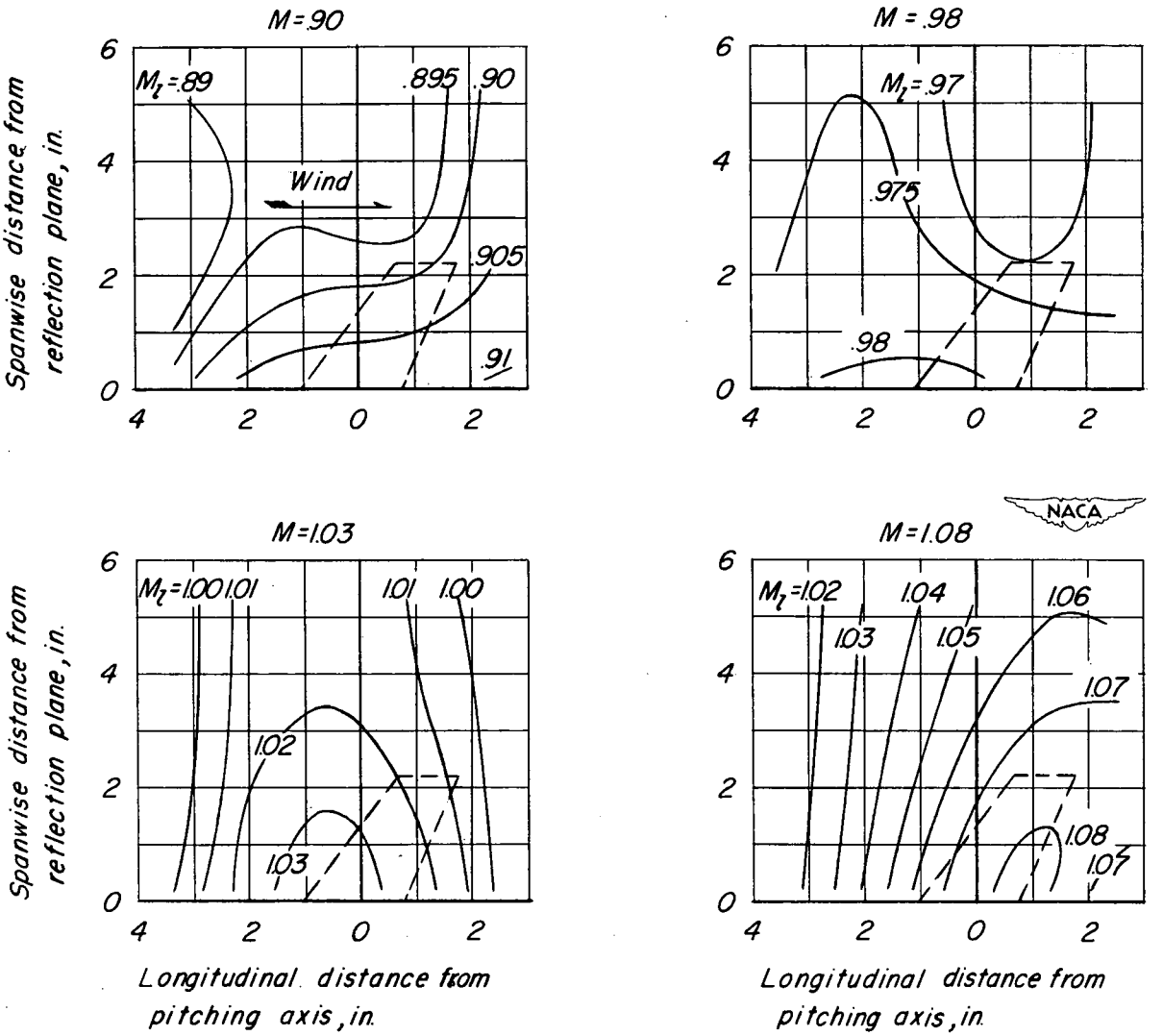

Figure 2.- Mach number distribution over reflection plane used for small-model tests.

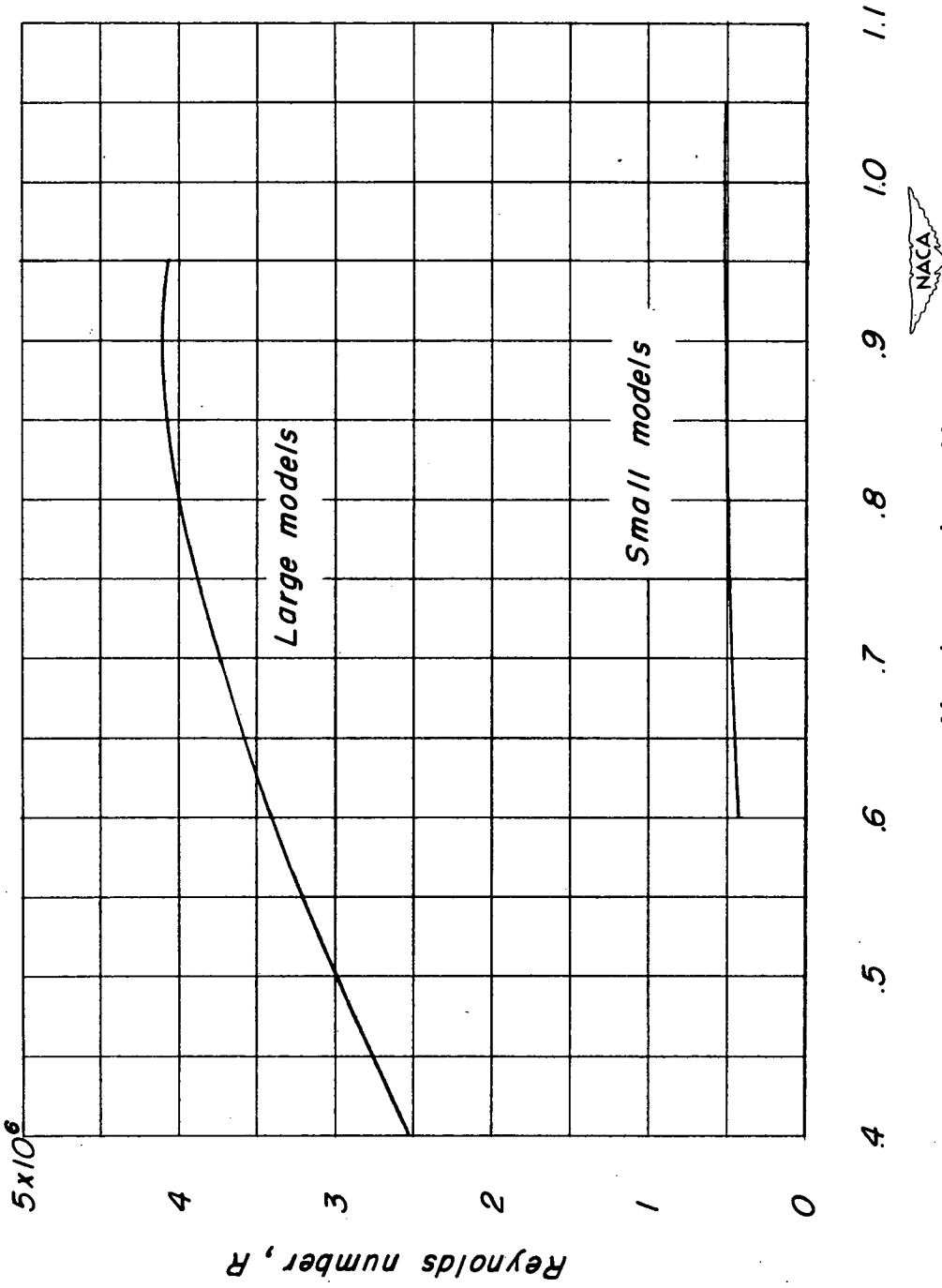

Figure 3.- Variation of Reynolds number with Mach number for average test conditions.

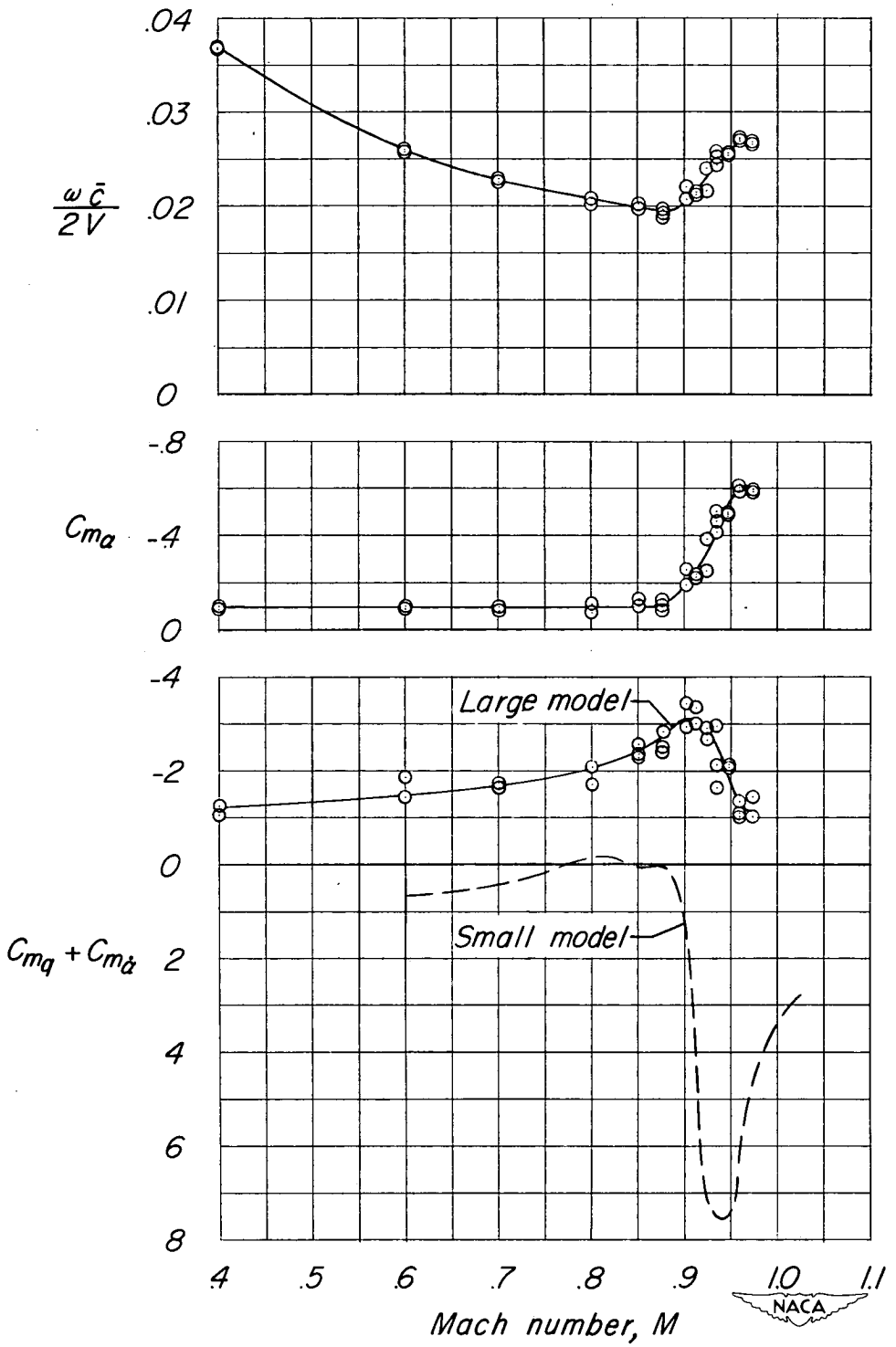

(a) $\frac{t}{c}$ = 0.06; smooth leading edge.

Figure 4.- Dynamic characteristics of test models.

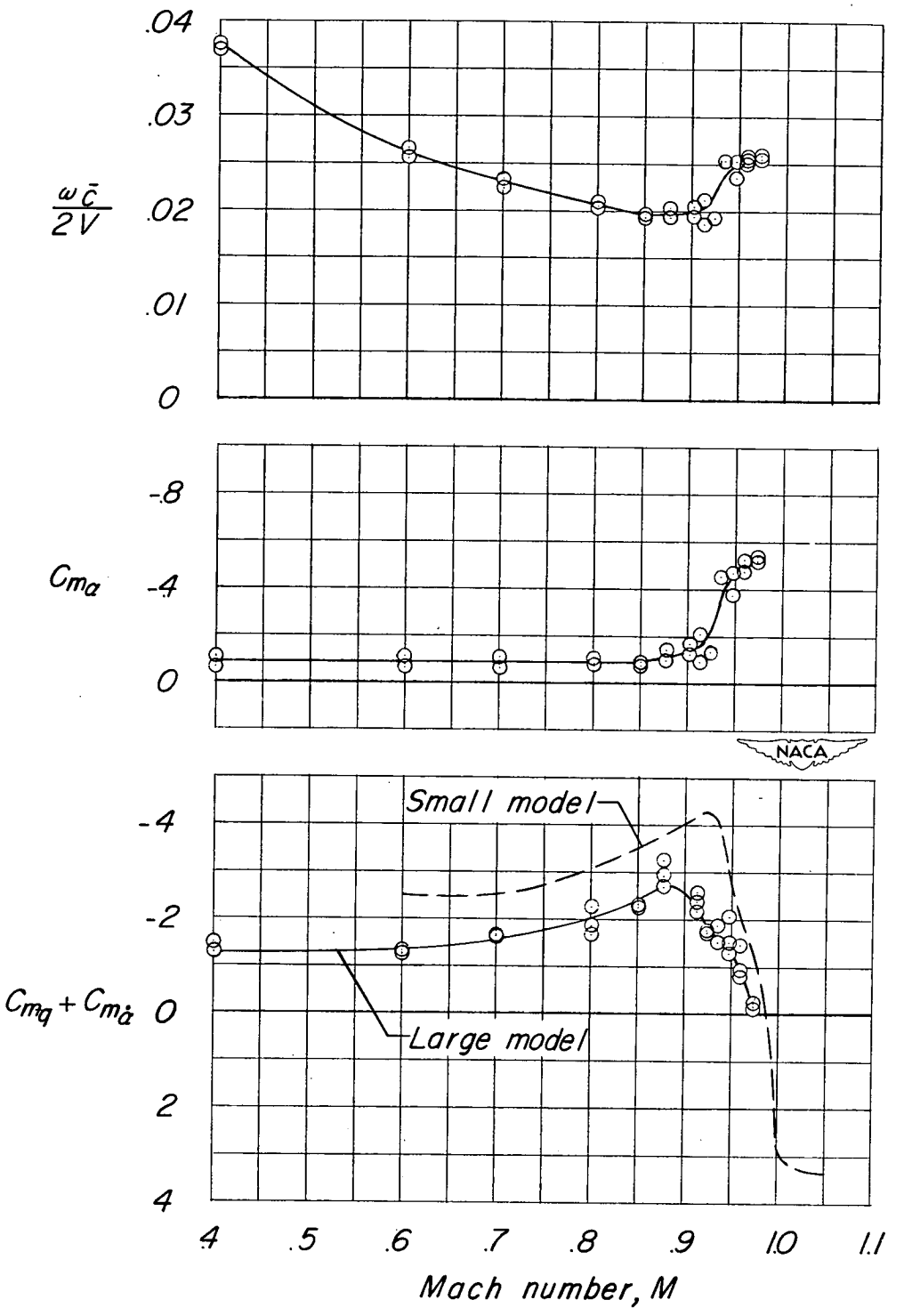

(b) $\frac{t}{c}$ = 0.06; rough leading edge.

Figure 4.- Continued.

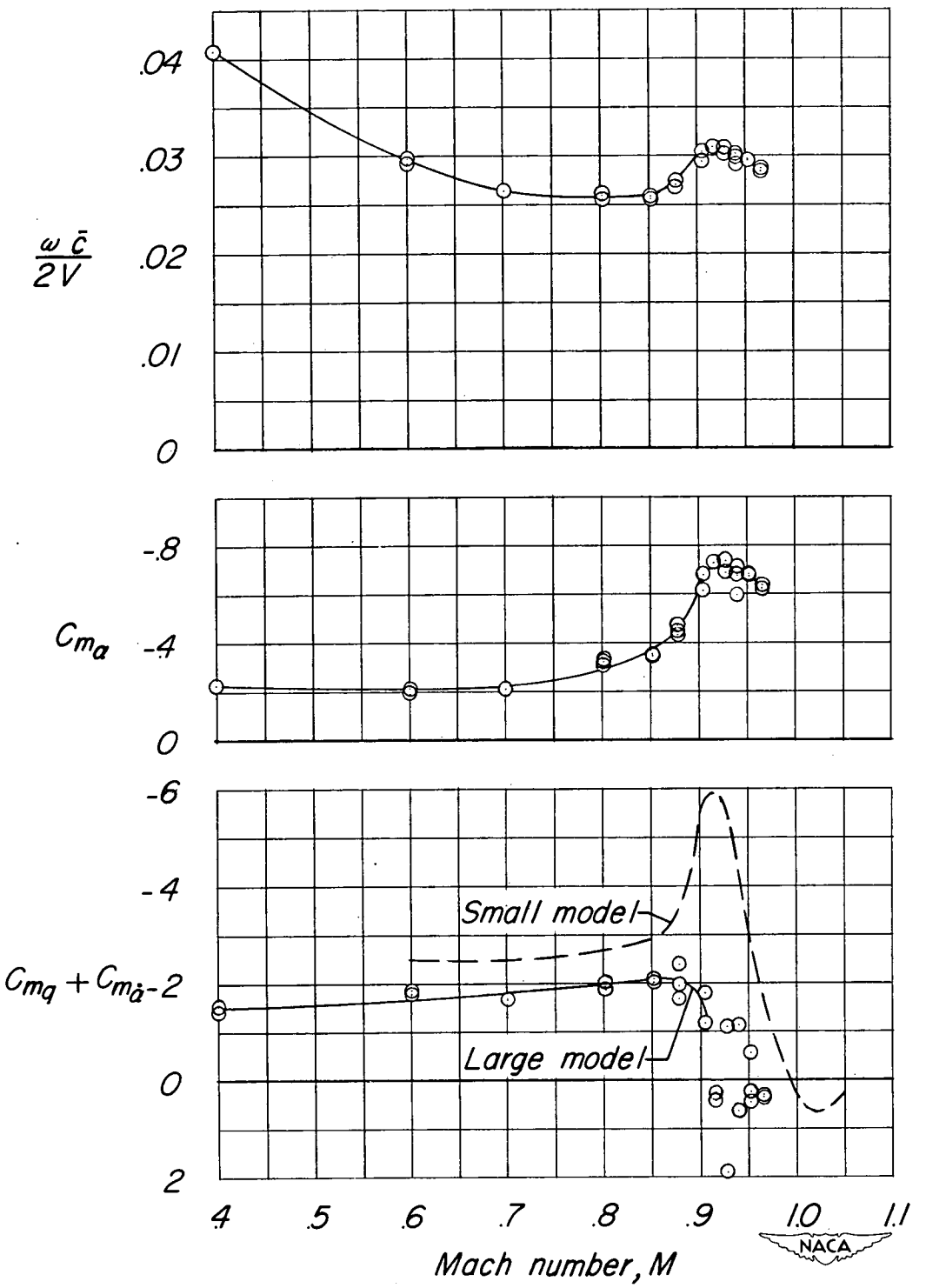

(c) $\frac{t}{c}$ = 0.105; smooth leading edge.

Figure 4.- Continued.

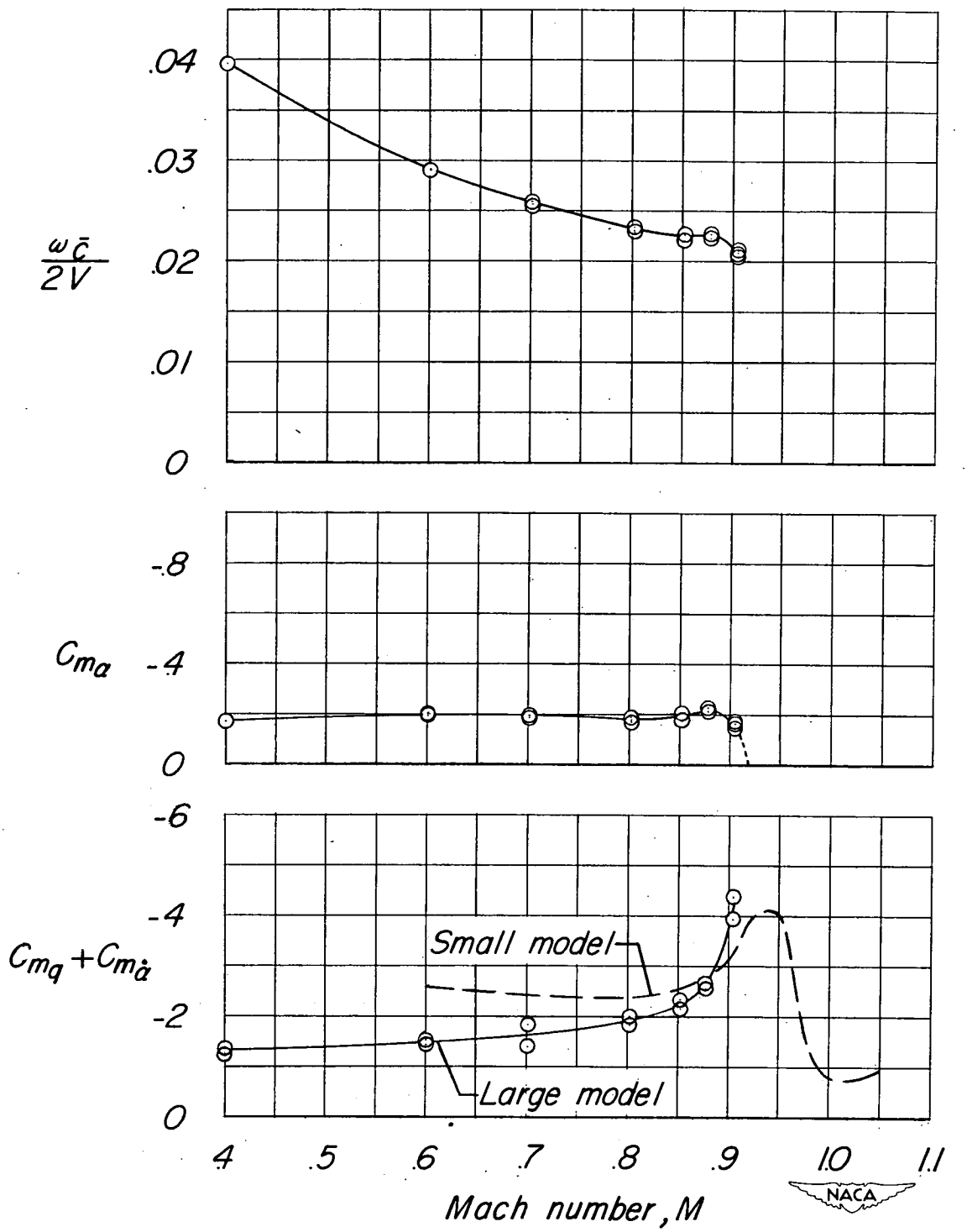

(d) $\frac{t}{c}$ = 0.105; rough leading edge.

Figure 4.- Continued.

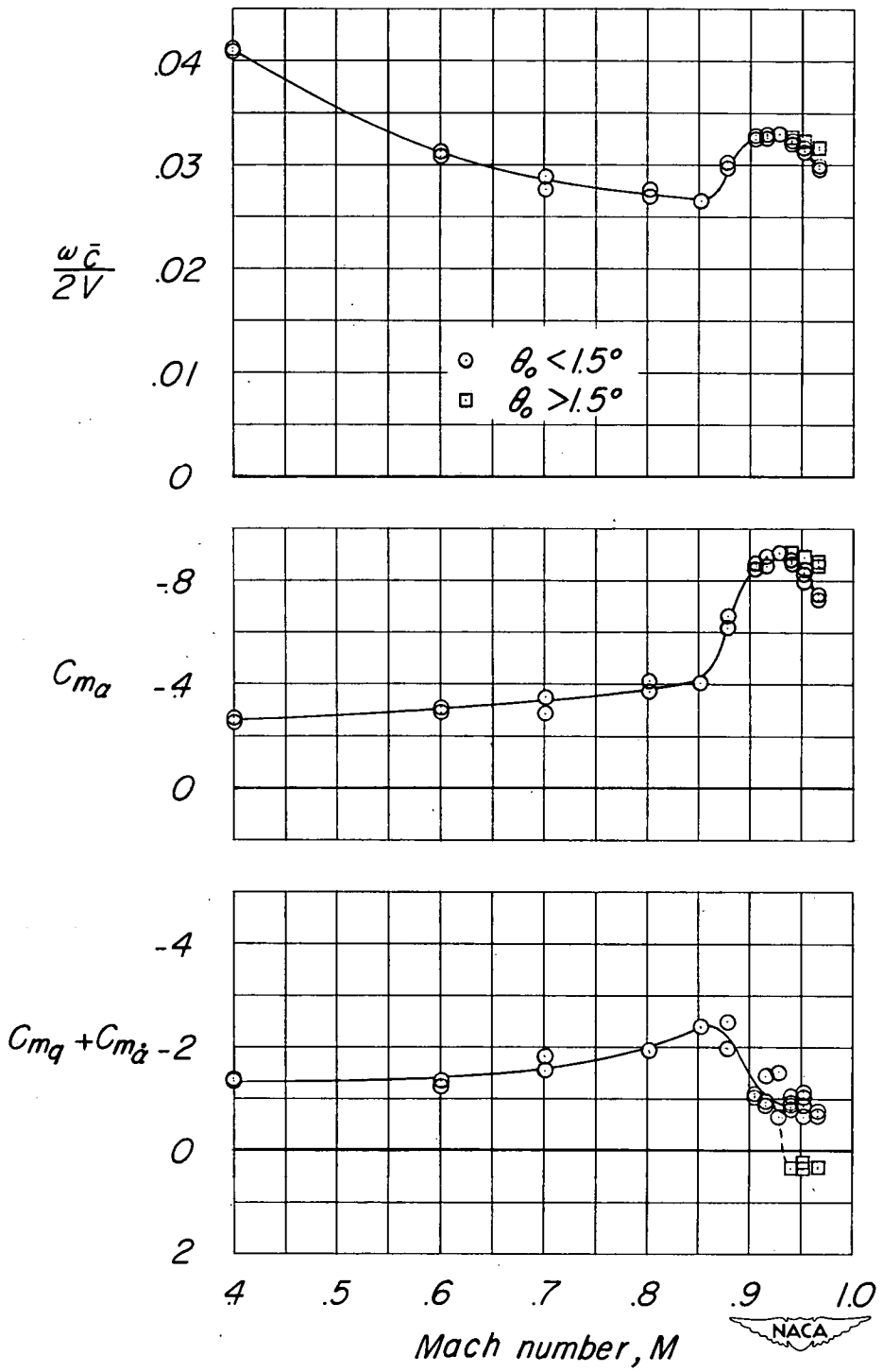

(e) $\frac{t}{c}$ = 0.105; smooth leading edge; trailing-edge strips.

Figure 4.- Concluded.

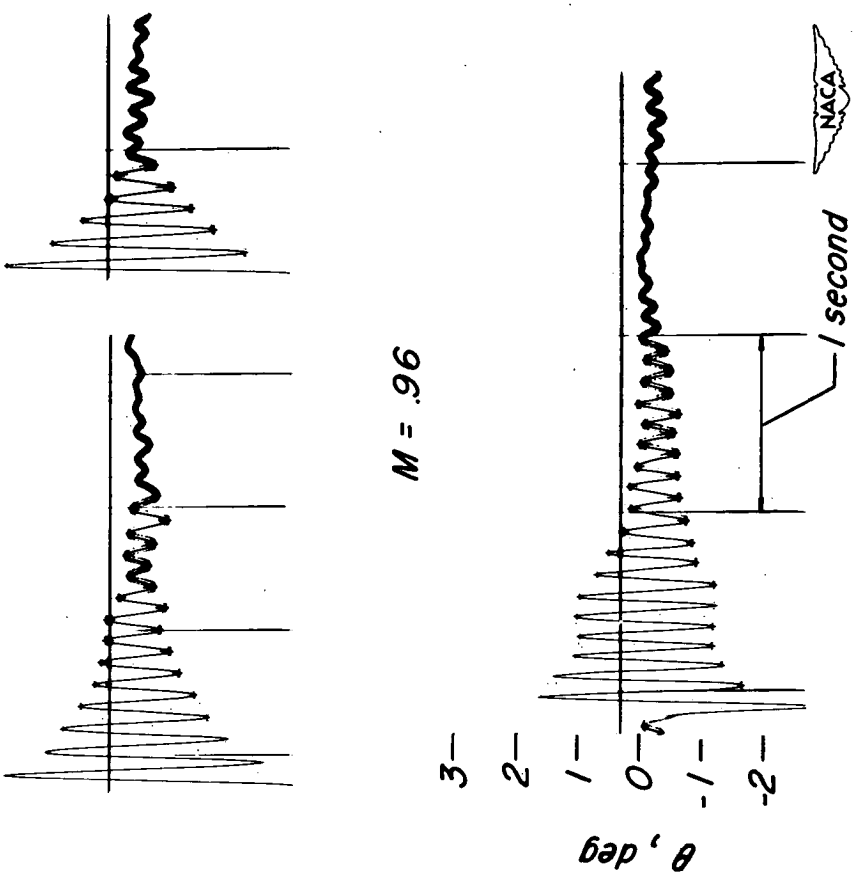

(a) $\frac{t}{c}$ = 0.06; smooth leading edge.

Figure 5.- Selected test records illustrating the effect of buffeting on motion of large models.

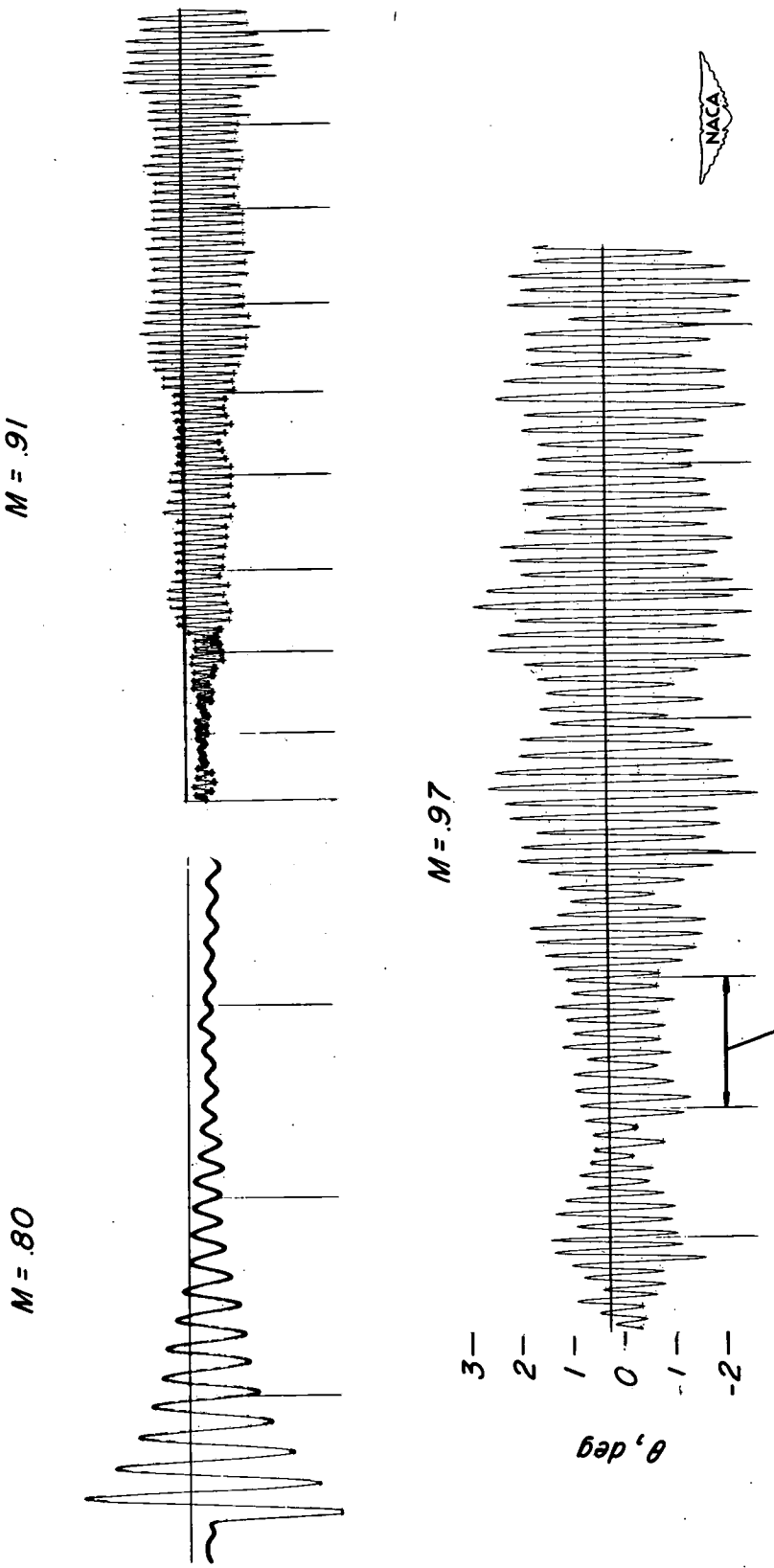

(b) $\frac{t}{c}$ = 0.105; smooth leading edge.

Figure 5.- Continued.

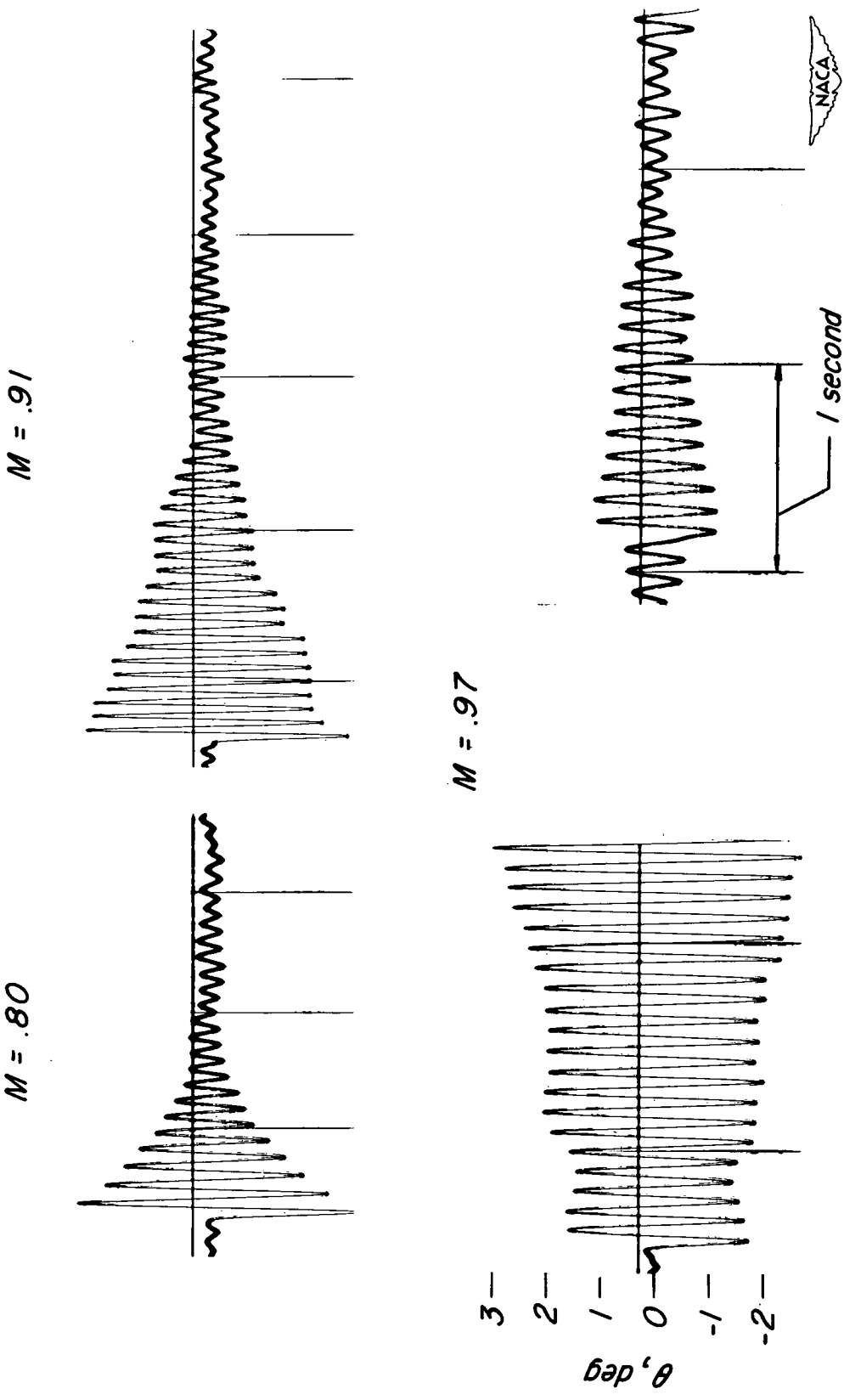

(c) $\frac{t}{c}$ = 0.105; smooth leading edge; trailing-edge strips.

Figure 5.- Concluded.

NACA-Langley - 10-16-53 - 325